



HAL
open science

Data acquisition in Thermodynamic and electrochemical reduction in a Gd(III)/Gd system in LiF-CaF₂ media

Christophe Nourry, Laurent Massot, Pierre Chamelot, Pierre Taxil

► To cite this version:

Christophe Nourry, Laurent Massot, Pierre Chamelot, Pierre Taxil. Data acquisition in Thermodynamic and electrochemical reduction in a Gd(III)/Gd system in LiF-CaF₂ media. *Electrochimica Acta*, 2008, vol. 53 (n° 5), pp.2650-2655. 10.1016/j.electacta.2007.10.050 . hal-03580112

HAL Id: hal-03580112

<https://hal.science/hal-03580112>

Submitted on 26 Mar 2024

HAL is a multi-disciplinary open access archive for the deposit and dissemination of scientific research documents, whether they are published or not. The documents may come from teaching and research institutions in France or abroad, or from public or private research centers.

L'archive ouverte pluridisciplinaire **HAL**, est destinée au dépôt et à la diffusion de documents scientifiques de niveau recherche, publiés ou non, émanant des établissements d'enseignement et de recherche français ou étrangers, des laboratoires publics ou privés.

Data acquisition in Thermodynamic and electrochemical reduction in a Gd(III)/Gd system in LiF-CaF₂ media

C. Nourry, L. Massot*, P. Chanelot and P. Taxil

Laboratoire de Génie Chimique UMR 5503, Département Procédés Electrochimiques,

Université Paul Sabatier, 31062 Toulouse Cedex9, France

(*) corresponding author:

Massot Laurent

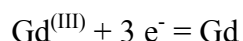
Tel : + 33 (0) 5 61 55 81 94

fax : + 33 (0) 5 61 55 61 39

E-mail : massot@chimie.ups-tlse.fr

Abstract

The electrochemical reduction of GdF_3 was studied in the LiF-CaF_2 eutectic (77/23 mol%) on a tantalum electrode for various GdF_3 concentrations in the 800-900°C temperature range. A previous thermodynamic study showed that gadolinium trifluoride is reduced to metal in a one-step process:



Cyclic voltammetry and square wave voltammetry were used to confirm this mechanism, and the results show that the electrochemical reduction process is limited by the diffusion of $\text{Gd}^{(\text{III})}$ in the solution.

The $\text{Gd}(\text{III})$ diffusion coefficient was calculated at different temperatures and the results obey the Arrhenius law with an activation energy of $83 \pm 4 \text{ kJ}\cdot\text{mol}^{-1}$.

The activity coefficient of $\text{Gd}^{(\text{III})}$ and the $\text{Gd}^{(\text{III})}/\text{Gd}$ standard potential E° were determined in the melt at various temperatures and concentrations. The values obtained for the activity coefficients were close to 1 at the highest temperatures and between 1.3 and 1.6 at lower temperatures.

Key words

Molten fluorides, gadolinium, cyclic voltammetry, electrochemistry, extraction.

1. Introduction

Nowadays, in France, partitioning and reprocessing of spent nuclear fuel are performed with hydrometallurgical methods such as the PUREX process. These methods will not be

appropriate to treat the waste of future nuclear reactors due to the inertness of the matrix containing the fuel which cannot be completely dissolved in aqueous media. So, alternative types of solvent have to be proposed. Molten salts and more particularly molten fluorides seem to exhibit suitable solvent properties for these processes.

Fission reactions release lanthanides. Since these elements are neutron absorbers their selective extraction from the salt is a requisite. One of the possible ways to extract lanthanide ions from molten fluorides is their electrochemical reduction to metal on a cathode. To operate the extraction process the electrochemical system involved must be investigated beforehand.

Gadolinium is one of the fission products. This work deals with the electrochemical behaviour of gadolinium in the LiF-CaF₂ eutectic in the 800-900°C temperature range with a tantalum electrode.

Yang *et al.* [1] studied Gd^(III) reduction in NaCl-KCl at 730°C and in KCl at 800°C. The studies showed that Gd^(III) reduction proceeds in a single step, which is diffusion controlled:



In NaCl-KCl, the Gd^(III) diffusion coefficient calculated by these authors was $2.5 \cdot 10^{-5} \text{ cm}^2 \text{ s}^{-1}$ at 730°C and $3.6 \cdot 10^{-5} \text{ cm}^2 \text{ s}^{-1}$ in KCl at 800°C.

Iizuka [2] determined the variation of the Gd^(III) diffusion coefficient as a function of temperature in LiCl-KCl:

$$\log D = -2.78 - \frac{1670}{T} \quad (2)$$

More recently, the reduction of Gd^(III) was investigated in molten fluorides (LiF-NaF-KF, in the eutectic composition (FLINAK)) by Shim *et al.* [3] and Zvejskova *et al.* [4] in the same temperature range (550 and 527 °C respectively). The results that these authors obtained were not in complete agreement; they did agree that the reduction of Gd^(III) proceeds in two steps:





Nevertheless, according to Shim *et al.* the second step is observed prior to solvent reduction (at a 270 mV more cathodic potential than reaction (3)) while Zvejskova *et al.* pointed out a difference of about 1.06V between the two following steps, which shifts reaction (4) to a more cathodic potential than the solvent reduction.

These results will be compared with our own in the present study. In the first part of the study, the potential-oxoacidity diagram of gadolinium was examined in order to yield thermodynamic data concerning the $\text{Gd}^{(\text{III})}$ reduction mechanism while the second part concerned with the experimental and detailed study of the reduction mechanism in LiF-CaF_2 media using electrochemical techniques.

2. Experimental

The experimental cell consisted of a glassy carbon crucible (Carbone Lorraine V25) containing the electrolyte bath; the crucible was introduced in a cylindrical vessel made of refractory steel. The inner part of the vessel was protected against fluoride vapour by a graphite liner. The top of the cell was cooled with circulating water and the cell was placed under argon atmosphere (U grade, less than 5 ppm O_2). A more detailed description of our experimental set up can be found in ref [5;6].

The solvent used as electrolytic bath was the eutectic LiF/CaF_2 (Merk suprapur 99.99%) (77/23 molar percent): melting point 762°C . Before each experiment, the salt mixture was dehydrated by heating under vacuum up to melting point.

Gadolinium trifluoride GdF_3 (Alpha Aesar 99.99%) was used as solute and was introduced into the melt in the form of pellets.

Ta (1-mm diameter) (Goodfellow 99.95%) wires immersed in the electrolyte on about 1cm were used as working electrode.

The auxiliary electrode was a glassy carbon rod (Carbone Lorraine V25) with a large surface area (2.5 cm²).

The potentials were referred to a platinum wire (0.5 mm diameter) immersed in the molten electrolyte. According to [7], this electrode acts as a quasi-reference electrode Pt/PtO_x/O²⁻ with a stable potential depending on the residual [O²⁻] content of the bath, which is assumed to be invariable during our experiments.

Cyclic voltammetry and square wave voltammetry were used to investigate the electrochemical system. An Autolab PGSTAT30 potentiostat / galvanostat controlled by a computer using the research software GPES 4.9 was used to perform these techniques.

3. Results and discussion

3.1. Analysis of the gadolinium E- p_{CaO} diagram

The gadolinium E- p_{CaO} diagram, shown in figure 1, exhibits the stability zones of each species containing gadolinium associated with oxygen or fluorine in a LiF-CaF₂ medium (only GdF_{3(dissolved)}, Gd₂O_{3(s)} and Gd_(s) were taken into account), versus the potential and p_{CaO} which is representative of the oxide content in the bath. This diagram was plotted at 800°C (1073 K) using HSC 4.1 software and the activities of all soluble species were taken as equal to 0.1.

This diagram predicts that GdF_3 is reduced into $\text{Gd}(0)$ in a one-step process, GdF_3/Gd which can obviously be written as:



This reaction occurs at a potential that is less cathodic than the solvent reduction ($\text{Li}^+ + e^- = \text{Li}$), proving that it is possible to produce gadolinium metal on an inert electrode in LiF-CaF_2 medium.

The diagram also shows that at relatively high oxygen contents ($p\text{CaO} \approx 3$), GdF_3 will precipitate into Gd_2O_3 . This emphasizes the necessity of controlling the oxide content in the bath in order to prevent the precipitation of gadolinium oxide.

The following part of this article concerning the electrochemical study of GdF_3 reduction on an inert electrode, confirmed the above assumption

3.2. The mechanism of GdF_3 reduction on an inert electrode

3.2.1 Cyclic voltammetry

Cyclic voltammetry was carried out on a tantalum electrode at 800°C . Figure 2 shows a typical cyclic voltammogram obtained in a $\text{LiF-CaF}_2\text{-GdF}_3$ (0.14 mol.kg^{-1}) system. Tantalum was chosen as working electrode because of its inertness with respect to gadolinium at the working temperature. It exhibits one cathodic peak (at -1.7 V) prior to solvent reduction (Li^+). In these experimental conditions, the potential difference between the two reactions, ΔE , is estimated to be 0.2V . The associated reoxidation signal exhibits the shape of a stripping peak, that indicates that the reduction product is a solid phase. Furthermore, at constant temperature, the cathodic peak current density increases linearly when the GdF_3 concentration

increases as shown in Figure 3. Consequently, the cathodic peak can be associated to $Gd^{(III)}$ ion reduction into Gd metal.

The peak intensity was also correlated to the potential scan rate by using the Berzins Delahay relation, relevant for a reversible soluble/insoluble system [8]:

$$I_p = -0.61 n F S C \sqrt{\frac{nF}{RT} D r} \quad (6)$$

where n is the number of exchanged electrons, F the Faraday constant, S the electrode surface area in cm^2 , C the solute concentration in $mol.cm^{-3}$, T the temperature in K, D the diffusion coefficient in $cm^2.s^{-1}$, r the potential scan rate in $V.s^{-1}$.

Figure 4 exhibits the evolution of the peak intensity versus the square root of the scan rate. The linear relationship observed on this figure validates equation (6) for the Gd^{III}/Gd system in our experimental conditions and proves that the electrochemical process was controlled by the diffusion of $Gd^{(III)}$ in solution.

3.2.2 Determination of the number of exchanged electrons

The electrochemical method used to determine the number of exchanged electrons was square wave voltammetry [9;10]. In this technique, the potential scan proceeds step by step with superimposition, on each step of the staircase, of two successive potential pulses, direct and reverse, of the same intensity. Plotting the differential intensity measured at each step between the successive pulses, versus the potential, provides a peak with a Gaussian shape associated to each electrochemical reaction. The mathematical analysis of the peak yields, for an electrochemical system in conditions of reversibility, a simple equation associating the half-width of the peak $W_{1/2}$ and the number of electrons exchanged:

$$W_{1/2} = 3.52 \frac{RT}{nF} \quad (7)$$

This equation is valid only if the reversibility criteria are verified by the electrochemical system. In previous works [5;11-12] we assumed that the linearity of the current peak with the square root of the frequency of the signal was a determining factor for applying eq. (7).

Figure 5 shows a typical square wave voltammogram of GdF_3 reduction in $LiF-CaF_2$ on a tantalum electrode at $800^\circ C$ and a frequency of 9Hz. We can observe in this figure one peak at around -1.6 V vs. Pt. As specified above, the validity of eq. (7) was tested by plotting the peak current density versus the square root of the signal frequency. Linearity was observed in a 9-64 Hz frequency range as seen in Figure 6. We conclude that eq. (7) is valid when the square wave voltammogram is drawn at 9Hz. The use of the lower values of the validity domain is preferable because low frequencies, improve curve precision.

The peak observed (fig.5) is not symmetrical as it could have been. This feature had already been observed in our laboratory for other reduction process leading to a metal deposition; it was attributed to a nucleation effect [13, 14]. The width at half height ($W_{1/2}$) was therefore calculated by doubling the value of the left side of the peak determinate graphically ($2 W_L$) as in figure 5.

The measurements of W_L and W_R give two relevant results concerning the electrochemical system $Gd^{(III)}/Gd$:

- The nucleation overvoltage η , which is measured by the voltage gap between the simulated beginning of the current increase without the changing phase and the one observed.

According to this, η is given by the following equation:

$$\eta = 2(W_L - W_R) \quad (8)$$

In the present system we found that η was equal to 90 ± 5 mV. Other authors have found results of the same order of magnitude for the nucleation overvoltage of the electrodeposition system in molten salts using a chronopotentiometric method [15-17].

- The number of electrons exchanged was calculated using (3) with $W_{1/2} = 2 W_L$, calculated from fig. 5 (the left part of the peak was not influenced by the nucleation effect) and had a value of 3.01. Ten measurements led to an average value of 3 ± 0.05 . This confirms that the electrochemical reduction mechanism of Gd(III) involves a single step. There is a discrepancy between our results and those obtained in molten fluorides by ref [3] and [4] which is probably due to the difference in working temperature (more than 300°C).

3.2.3 Determination of diffusion coefficient

Using equation (6) with $n = 3$, the Gd^(III) diffusion coefficient (D) was calculated and found to be $1.25 \pm 0.3 \cdot 10^{-5} \text{ cm}^2 \cdot \text{s}^{-1}$ at 800°C.

Using the same method, the Gd^(III) diffusion coefficient was determined at other temperatures in the 800-900°C range. The results are reported in Table 1.

The variation of Ln D versus the inverse absolute temperature is plotted in Figure 7. The linear relationship between Ln D and 1/T observed proved that the variation of the diffusion coefficient obeys an Arrhenius law:

$$D = D^{\circ} \exp\left(-\frac{E_a}{RT}\right) \quad (9)$$

Where E_a is the activation energy in $\text{kJ} \cdot \text{mol}^{-1}$, T is the temperature in K, D is the diffusion coefficient in $\text{cm}^2 \cdot \text{s}^{-1}$.

The results obtained give the following equation:

$$\ln D = -2.1867(\pm 0.5) - \frac{9984.8(\pm 500)}{T} \quad (10)$$

Using this equation we found that, the activation energy was $83 \pm 4 \text{ kJ mol}^{-1}$.

3.3. Thermodynamic properties

3.3.1 Determination of GdF_3/Gd standard potential as a function of temperature

According to the Nernst Law the reduction potential of Gd^{III} into Gd is expressed as follows:

$$E = E^\circ_{\text{GdF}_3/\text{Gd}} + \frac{RT}{3F} \ln \gamma_{\text{GdF}_3} + \frac{RT}{3F} \ln C_{\text{GdF}_3} \quad (11)$$

where γ_{GdF_3} and C_{GdF_3} are the activity coefficient and the concentration of solved GdF_3 respectively.

E was determined using the cyclic voltammogram of GdF_3 in the molten fluoride solution with a potential scale using the F_2/F^- system as reference:

$$E = E_{\text{Li}} + \Delta E \quad (12)$$

where E_{Li} was calculated using HSC 4.1 software, with reference to the F_2/F^- system and ΔE was determined using the cyclic voltammogram as shown in figure 2.

According to (11), $E - \frac{RT}{3F} \ln C_{\text{GdF}_3} = E^\circ_{\text{GdF}_3/\text{Gd}} + \frac{RT}{3F} \ln \gamma_{\text{GdF}_3}$, so at a given temperature, it

was possible to determine the GdF_3/Gd standard potential (E°) by extrapolating the

experimental value of $\left(E - \frac{RT}{3F} \ln C_{\text{GdF}_3} \right)$ versus C_{GdF_3} when C_{GdF_3} tends towards 0; indeed,

at infinite dilution $\gamma = 1$ (see figure 8) [18].

The results of a series of measurements of E° were obtained at 800, 833, 866 and 900°C and allowed plotting the variation of E° versus the temperature (see Figure 9). The linearity

between E° and T means that the standard enthalpy of the dissolved species ΔH_s° and the standard entropy ΔS_s° are constant in the considered temperature range:

$$E^\circ_{\text{GdF}_3/\text{Gd}} = A + BT \quad (13)$$

$$\text{where } A = \frac{\Delta H_s^\circ}{3F} \text{ and } B = -\frac{\Delta S_s^\circ}{3F}.$$

Using the linear relationship determined from figure 9, the values obtained are: $\Delta H^\circ = -1635.26 \pm 100 \text{ kJ}\cdot\text{mol}^{-1}$ and $\Delta S^\circ = -153 \pm 30 \text{ J}\cdot\text{mol}^{-1}$.

Consequently it is possible to calculate the Gibbs energy of the GdF_3 dissolved species:

$$\Delta G_s^\circ = \Delta H_s^\circ + T \Delta S_s^\circ \quad (14)$$

The difference between the Gibbs energy of crystallised GdF_3 , $\Delta_f G^\circ$ and ΔG_s° , is the free energy of the solvation reaction of GdF_3 in the fluoride solution:



The free energy of reaction (15) $\Delta_f G^\circ$ is called transfer energy. Determining $\Delta_f G^\circ$ using HSC 4.1 software, allows ΔG°_t calculations which are reported in table 2. The values between -36.60 and -43.93 kJ mol^{-1} in the 800-900°C (1073-1173 K) temperature range were lower than the transfer energy of GdCl_3 in LiCl-KCl found to be -50.93 kJ mol^{-1} at 477°C (750 K) by Lantelme *et al.*[18].

3.3.2 Determination of GdF_3 activity coefficient

The GdF_3 activity coefficient (γ_{GdF_3}) was calculated using the following equation derived from eq. 11:

$$\gamma_{\text{GdF}_3} = \exp\left(\frac{3F}{RT}\left(E - \left(E^\circ + \frac{RT}{3F}\text{Ln}(C_{\text{GdF}_3})\right)\right)\right) \quad (15)$$

This calculation was performed for concentrations up to 0.19 mol kg⁻¹ and at 800, 833, 866 and 900°C. The obtained results are reported in Table 3. The values are close to 1, meaning that for this temperature and concentration range, the behaviour of GdF₃ in the melt is close to ideal.

3.3.3 Use of thermodynamic data for predicting the extraction efficiency

Combining the knowledge of $E^{\circ}_{\text{Gd}^{\text{III}}/\text{Gd}}$ and γ calculated in this work allows the determination of the equilibrium potential of the Gd^{III}/Gd system using eq. 11.

If the extraction efficiency is called X,

$$X = \frac{C_i - C_f}{C_i} \quad (16)$$

Where C_f and C_i are the final and initial Gd^{III} concentration (mol kg⁻¹) respectively.

The working electrode potential at the end of electrolysis is:

$$E_f = E^{\circ} + \frac{RT}{3F} \text{Ln}((1-X)C_i) \quad (17)$$

Assuming that $\gamma = 1$ at the end of the extraction, taking into account the required value of X (99.99%), for a complete extraction we must have

$$E_f > E_{\text{Li}^+/\text{Li}} \quad (18)$$

For example, with $C_i = 0.068$ mol kg⁻¹ which is the right order of magnitude for lanthanide concentrations in nuclear wastes, at 833°C, $E_f = -5.45$ V; but, at this temperature, $E_{\text{Li}^+/\text{Li}} = -5.31$ V. According to eq. 18 this result is not satisfactory since it shows that the required extraction efficiency of 99.99% cannot be obtained with an inert cathode.

3. Concluding remarks

The determination of E° and γ for the Gd^{III}/Gd system in molten fluorides is of great importance because it allows the equilibrium potential of Gd ions in the molten salt mixture to be calculated accurately.

Calculations proved that the complete extraction of the lanthanide element (99.99%) is not possible by electrodeposition on an inert cathode. Alternatively, the use of a reactive cathode should avoid these drawbacks, as proved for similar extractions in our laboratory [19, 20]:

(i) this kind of electrode (Ni, Cu) reacts with the reducing ions to give alloys or compounds at potentials clearly lower than that of the pure metal

(ii) the alloy coatings are yielded within the cathodic matrix and are thus easier to recover.

Acknowledgments

The authors express their thanks to the PACE program (PCR RSF Thorium and GDR Paris) for financial support for this work.

References

- [1] Q. Yang, G. Liu, Y. Ao, *Proceedings – Electrochem. Soc.*, **94**(13) (1994) 498.
- [2] M. Iizuka, *J. Electrochem. Soc.*, **145**(1) (1998) 84.
- [3] J-B. Shim, S-C. Hwang, E-H. Kim, Y-H. Kang, B-J. Lee, J-H. Yoo, *Proceeding of the Seventh Information Exchange Meeting on Actinide and Fission Product Partitioning and Transmutation*, Jeju (Republic of Korea), (2002)
- [4] R. Zvejskova, P. Soucek, F. Lisy, J. Uhlir, *Proceeding of “InWor for P&T and ADS”*, Mol, Belgium, October 6-8, (2003)
- [5] P. Chamelot, B. Lafage, P. Taxil, *Electrochim. Acta*, **39** (1994) 2571.
- [6] L. Massot, P. Chamelot, F. Bouyer, P. Taxil, *Electrochim. Acta*, **48** (2003) 465.
- [7] A. D. graves, D. Inman, *Nature*, **208** (1965) 481.
- [8] T. Berzins, P. Delahay, *J. Am. Chem. Soc.*, **75** (1953) 555.
- [9] L. Ramaley, M.S. Krause, *Anal. Chem.*, **41** (1969) 1362.
- [10] J.G. Osteryoung, J.J. O'Dea, *Electroanal. Chem.*, **14** (1986) 209.
- [11] P. Chamelot, B. Lafage, P. Taxil, *Electrochim. Acta*, **43** (1997) 607.
- [12] P. Chamelot, P. Palau, L. Massot, A. Savall, P. Taxil, *Electrochim. Acta*, **47** (2002) 3423.
- [13] C. Hamel, P. Chamelot, P. Taxil, *Electrochim. Acta*, **49** (2004) 4467.
- [14] K. Serrano, P. Taxil, *J. Appl. Electrochem.*, **29** (1999) 497.
- [15] P. Chamelot, B. Lafage, P. Taxil, *J. Electrochem. Soc.*, **143**(5) (1996) 1570.
- [16] L. Massot, P. Chamelot, F. Bouyer, P. Taxil, *Electrochim. Acta*, **48** (2003) 465.
- [17] G.J. Hills, D.J. Schiffrin, J. Thomson, *Electrochim. Acta*, **19** (1974) 657.
- [18] F. Lantelme, Y. Berghoute, *J. Electrochem. Soc.*, **146**(11) (1999) 4137.
- [19] L. Massot, P. Chamelot, P. Taxil, *Electrochim. Acta* **50** (2005) 5510.
- [20] C. Nourry, L. Massot, P. Chamelot, P. Taxil, *J. New Mat. Electrochem. Systems*, **10** (2007) 117.

Figures legends

Fig 1:

E - pCaO diagram made using HSC 4.1 software at $T = 800^{\circ}\text{C}$ (1073 K) and all soluble species activities equal to 0.1.

Fig 2:

Cyclic voltammogram in $\text{LiF-CaF}_2\text{-GdF}_3$ (0.14 mol.Kg^{-1}) at 800°C ; scan rate: 100 mV s^{-1} .

Working Electrode: Ta ($S=0.330 \text{ cm}^2$); Auxiliary Electrode: vitreous carbon; Quasi-reference Electrode: Pt.

Fig 3:

Linear relationship between the GdF_3 reduction peak current density and the GdF_3 concentration in the melt.

Fig. 4:

Linear relationship of GdF_3 reduction peak current density versus the square root of the scanning potential in $\text{LiF-CaF}_2\text{-GdF}_3$ (0.14 mol.Kg^{-1}) at $T = 800^{\circ}\text{C}$.

Working Electrode: Ta ($S=0.330 \text{ cm}^2$); Auxiliary Electrode: vitreous carbon; Quasi-reference Electrode: Pt

Fig. 5:

Square Wave Voltammogram of the $\text{LiF-CaF}_2\text{-GdF}_3$ melt. Frequency : 9 Hz, $T = 800^{\circ}\text{C}$.

Working Electrode: Ta ($S=0.330 \text{ cm}^2$); Auxiliary Electrode: vitreous carbon; Quasi-reference Electrode: Pt

Fig. 6:

Linear relationship of GdF_3 reduction peak current density versus the square root of the frequency in $\text{LiF-CaF}_2\text{-GdF}_3$ (0.14 mol.kg^{-1}) at $T = 800^\circ\text{C}$.

Fig.7:

Linear relationship of the logarithm of the GdF_3 diffusion coefficient versus the reciprocal of the absolute temperature.

Fig.8:

Relationship between $E-(RT/nF)\ln C$ versus C at different temperatures.

Fig.9:

Relationship between the GdF_3/Gd standard potential and the temperature.

Table 1:

Variation of the GdF_3 diffusion coefficient with the temperature.

Table 2:

ΔG°_t of GdF_3 versus temperature.

Table 3:

GdF_3 activity coefficient, γ , in solution.

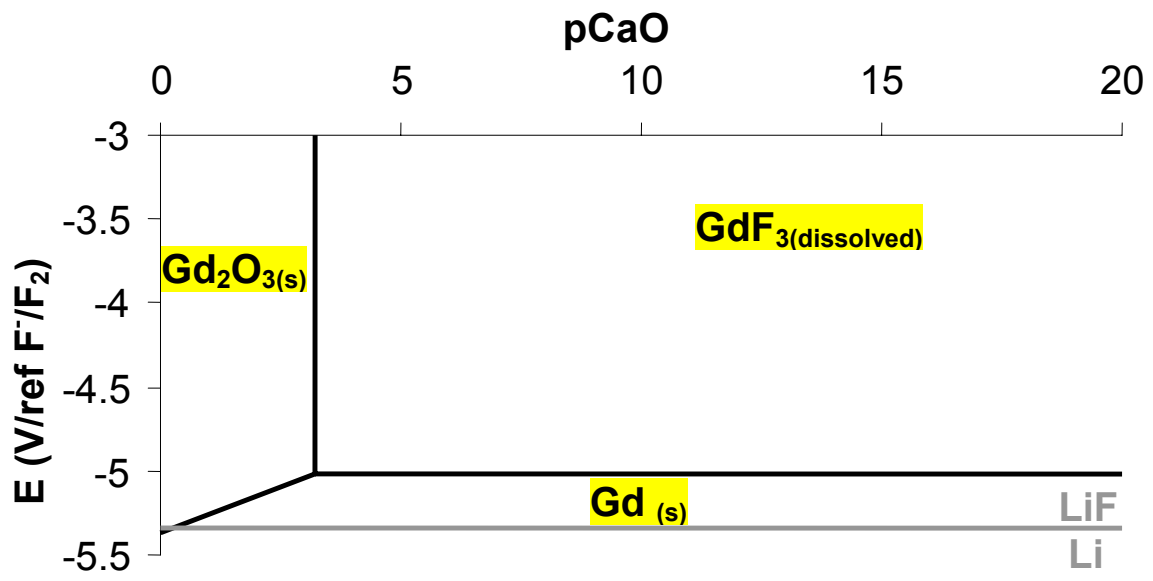


Figure 1

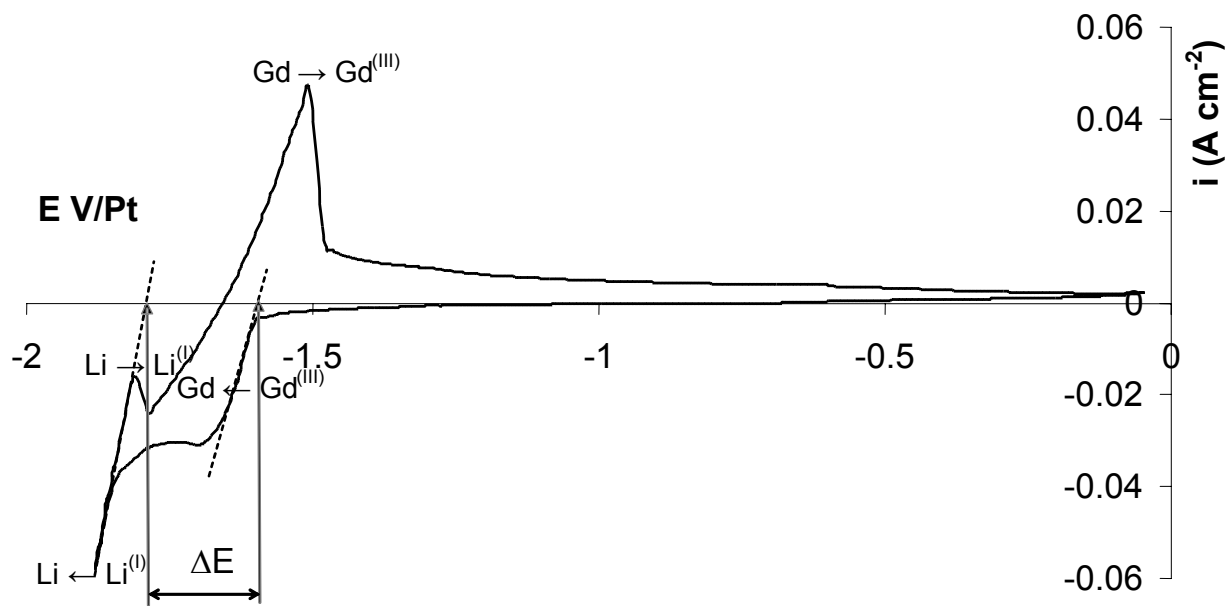


Figure 2

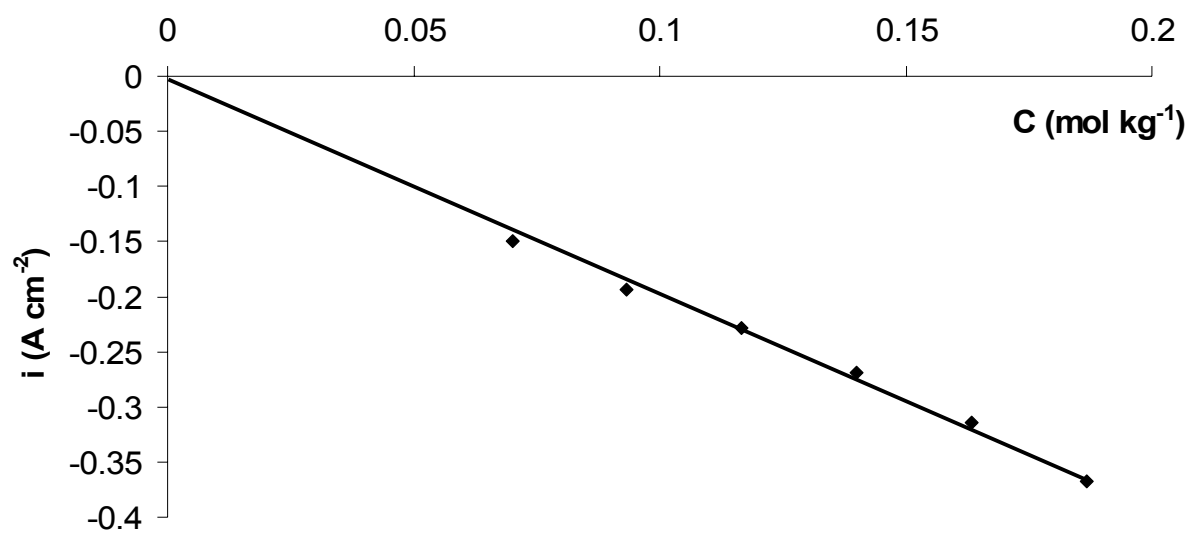


Figure 3

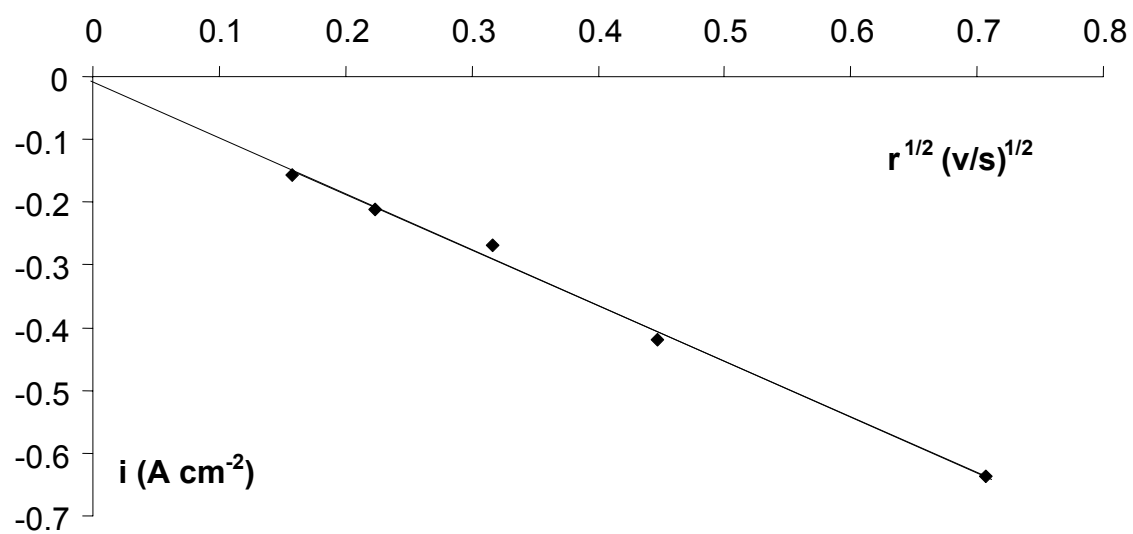


Figure 4

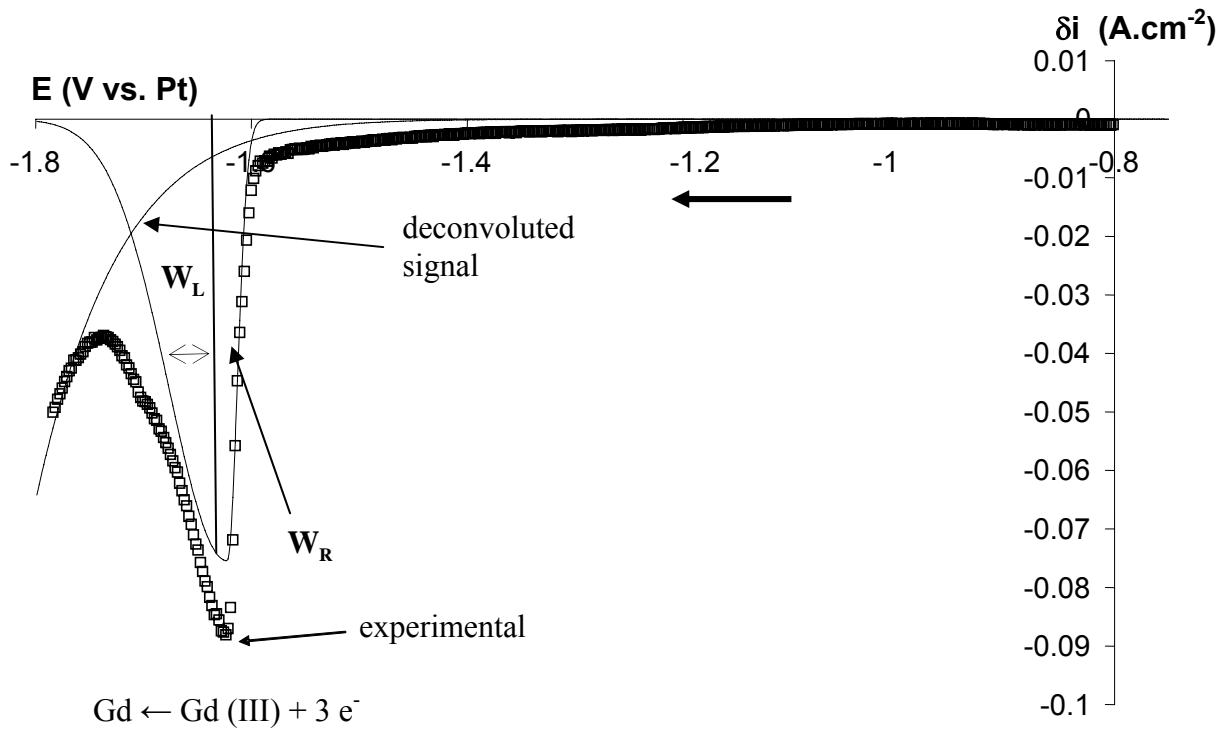


Figure 5

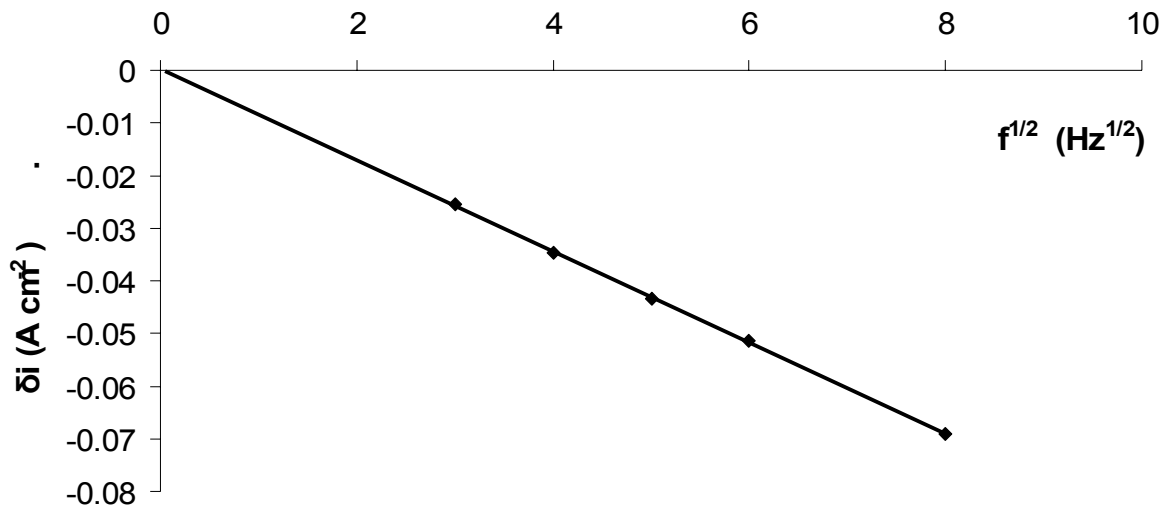


Figure 6

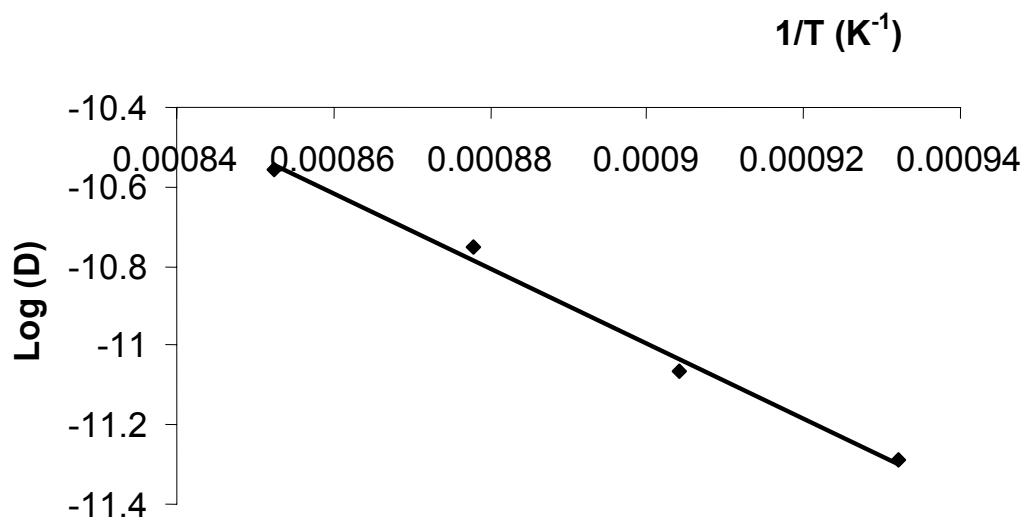


Figure 7

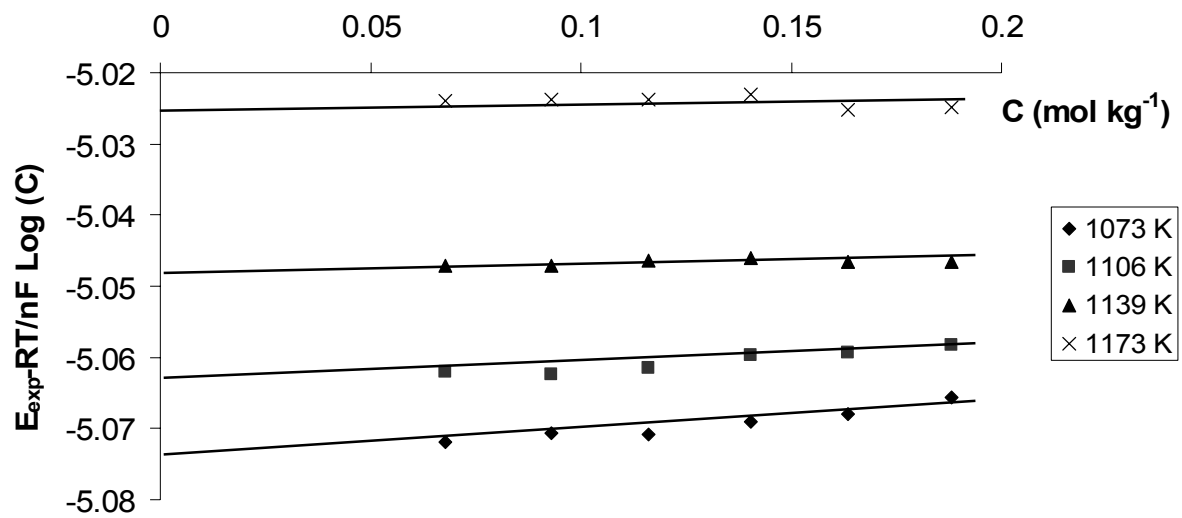


Figure 8

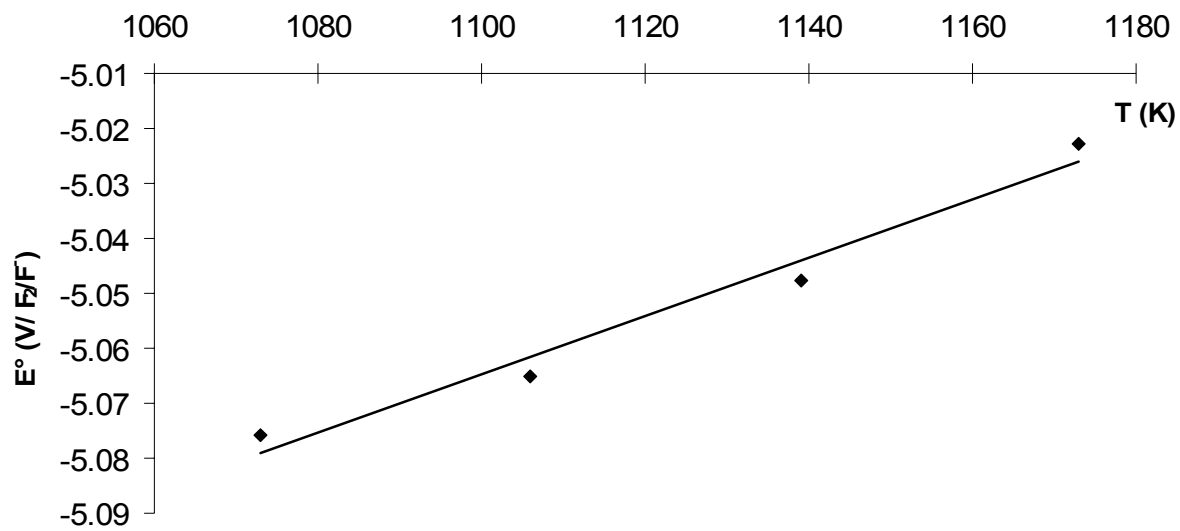


Figure 9

T (K)	D (cm ² s ⁻¹)
1073	1.249 10 ⁻⁵
1106	1.563 10 ⁻⁵
1139	2.144 10 ⁻⁵
1173	2.599 10 ⁻⁵

Table 1

	800°C	833°C	866°C	900°C
ΔG_t° (kJ mol ⁻¹)	-36.60	-39.04	-41.46	-43.93

Table 2

C mol kg ⁻¹	γ			
	800°C	833°C	866°C	900°C
0.068	1.16	0.89	0.80	0.92
0.093	1.21	0.88	0.80	0.93
0.116	1.20	0.91	0.82	0.93
0.140	1.28	0.96	0.83	0.95
0.163	1.33	0.97	0.82	0.89
0.188	1.43	1.00	0.82	0.90

Table 3